Sebaceous gland rich skin is characterized by TSLP expression and distinct immune surveillance which is disturbed in rosacea

Zsolt Dajnoki[1,2*], Gabriella Béke[1,2*], Anikó Kapitány[1,2], Gábor Mócsai[1,2], Krisztián Gáspár[1,2], Ralph Rühl[3,8], Zoltán Hendrik[4], István Juhász[2], Christos C. Zouboulis[9], Attila Bácsi[5], Tamás Bíró[5,6,7], Dániel Törőcsik[2] and Andrea Szegedi[1,2]

[1]Division of Dermatological Allergology, [2]Department of Dermatology, [3]MTA-DE Public Health Research Group of the Hungarian Academy of Sciences, Departments of [4]Pathology, [5]Immunology and [6]Physiology, [7]DE-MTA "Lendület" Cellular Physiology Research Group, Faculties of Medicine and Public Health, University of Debrecen, Debrecen, Hungary; [8]Paprika Bioanalytics Bt, Debrecen, Hungary; [9]Departments of Dermatology, Venereology, Allergology and Immunology, Dessau Medical Center, Dessau, Germany.

*These authors contributed equally to this work

Corresponding author: Andrea Szegedi, MD, PhD, Division of Dermatological Allergology, Department of Dermatology, Faculty of Medicine, University of Debrecen, Hungary, 4032, Nagyerdei street 98, Debrecen, Hungary, E-mail: aszegedi@med.unideb.hu

Key words: Thymic stromal lymphopoietin, skin immune system, dendritic cells, T cells, rosacea

Abbreviations used:

AD: Atopic dermatitis, Ab: Antibody, DC: Dendritic cell, EC: Epithelial cell, FA: Field area, IHC: Immunohistochemistry, Ig: Immunoglobulin, KCs: keratinocytes, MA: Mask area, MGG: May-Grünwald-Giemsa, ROI: Region of interest, PPR: Papulopustular rosacea, RT-PCR: quantitative real-time polymerase chain reaction, SGP: Sebaceous gland poor, SGR: Sebaceous gland rich, Th: T helper, TLR: Toll-like receptor, TSLP: Thymic stromal lymphopoietin

ABSTRACT

The microbial community exhibits remarkable diversity on topographically distinct skin regions, which may be accompanied by differences in skin immune characteristics. Our aim was to compare the immune milieu of healthy sebaceous gland rich (SGR) and sebaceous gland poor (SGP) skin areas, and to analyze its changes in an inflammatory disease of SGR skin. For this purpose, immunohistochemical, immunocytochemical and quantitative real-time PCR analyses of thymic stromal lymphopoietin (TSLP) and other cytokines, phenotypic immune cell markers and transcription factors were carried out in samples from SGP, SGR skin and from papulopustular rosacea (PPR). TSLP mRNA and protein production was also studied in cultured keratinocytes. In SGR skin, higher TSLP expression, dendritic cell (DC) appearance without prominent activation and T cell presence with interleukin (IL)-17/IL-10 cytokine milieu were detected compared to SGP skin. Linoleic acid, a major sebum component, was found to induce TSLP expression dose-dependently in keratinocytes. In PPR, significantly decreased TSLP level and influx of inflammatory DCs and T cells with IL-17/interferon-γ cytokine milieu were observed. According to our results, SGR skin is characterized by a distinct, non-inflammatory immune surveillance, which may explain the preferred localization of inflammatory skin diseases, and can influence future barrier repair therapeutic concepts.

INTRODUCTION

As an outstanding discovery of recent years, the microbial community has been shown to exhibit remarkable differences on topographically distinct skin areas (Grice et al., 2009; Grice and Segre, 2011). It has been demonstrated that colonization of these bacteria is dependent on the physiology of the skin site, as specific bacteria are being associated with moist, dry or sebaceous microenvironments, and the diversity of the chemical milieu in which these microbial communities live was also described (Bouslimani et al., 2015; Costello et al., 2009; Gao et al., 2007; Grice et al., 2009; Grice and Segre, 2011).

High-scale diversity of the microbiota was not only described on the skin barrier surface, but distinct sections of the gut are also known to be colonized by heterogeneous microbiota, which is associated with the different anatomical and physiological features of these sites (Eckburg et al., 2005). Besides the diversity of microbiota, recent studies indicated a mutual relationship between the host and these microorganisms, since they play important role in tissue homeostasis and local immunity (Belkaid and Segre, 2014; Maranduba et al., 2015; Naik et al., 2015). These assume the possibility that the level of immune activation may differ in distinct barrier surfaces, which has been already indicated in the gut. For example, thymic stromal lymphopoietin (TSLP), one of the major epimmunomes (epithelial cell-derived molecules which can instruct immune cells), was detected only in particular gut sections, with its highest, constitutive expression in colonic epithelial cells (ECs) (Rimoldi et al., 2005; Swamy et al., 2010). This protein is involved in the development of tolerance to commensal microflora through modulation of dendritic cell (DC) functions in the gut. The tolerogenic role of TSLP is supported by recent studies where decreased TSLP level and altered microbial composition were found in Crohn's disease (Podolsky, 2002; Round and Mazmanian, 2009). Until now, TSLP in the skin was only described under inflammatory conditions, such as

atopic dermatitis (AD) and psoriasis, and its only known function in this organ so far is the promotion of T helper (Th)2 polarizing DCs (He and Geha, 2010).

In this study, we asked the question whether the above topographical differences in skin microbiota and physiology can also be accompanied by topographical differences in skin immune activity and TSLP (epimmunome) production. The possibility that the skin immune system is characterized by distinct functional tuning on different skin regions was not challenged until now in the literature.

RESULTS

TSLP protein is constitutively expressed in SGR healthy skin, but almost absent from SGP healthy skin

To detect TSLP protein in topographically different skin regions, biopsies from sebaceous gland poor (SGP; representing dry areas) and sebaceous gland rich (SGR; representing seborrheic areas) healthy skin were obtained. Lesional skin of severe atopic dermatitis (AD) patients was used as positive controls for TSLP staining. To confirm immunohistochemistry (IHC) results three different antibodies (Abs) against TSLP were used (Figure 1a). In AD samples, strong TSLP positivity was detected in the granular and corneal but not in the basal and suprabasal layers of the epidermis. In all SGR skin biopsies, high TSLP expression was detected with all three anti-TSLP Abs in the epidermal keratinocytes (KCs), mainly in the upper epidermal layers, and in sebocytes of sebaceous glands (Table 1.). In contrast, in SGP samples, TSLP was completely or almost completely absent. Importantly, the intensity of TSLP staining (as assessed by Pannoramic Viewer software) was found to be significantly higher in SGR skin compared to SGP skin. However, TSLP expression in SGR skin was significantly lower than in AD skin (Figure 1a and b). TSLP protein levels were also measured in the stratum corneum by immunocytochemistry and were also found to be significantly elevated in SGR skin compared to SGP skin, but did not reach the level found in AD skin (Figure 1c). Interestingly, quantitative real-time PCR (RT-PCR) analysis detected nearly similar total TSLP mRNA expression in all skin types (SGR, SGP and AD skin) (Figure 1d).

Linoleic acid induces TSLP expression in keratinocytes

Sebum content, composition of commensal microbiota and UV radiation are able to influence SGR and SGP skin differently; therefore, the effects of these factors on TSLP production in HaCaT and NHEK cells were analyzed by using RT-PCR and ELISA. As similar TSLP

protein levels were detected in hairy scalp (UV-protected) and face (UV-exposed) biopsy samples (Table 1), we did not investigate further the effect of UV.

To study the effect of chitin – a major component of *Demodex folliculorum*, which is part of the normal skin flora in SGR skin – and sebum, HaCaT KCs were treated with chitin (Figure 2a), with supernatant of cultured human SZ95 sebocytes (Zouboulis et al., 1999) (Figure 2b) and with different lipid components of sebum (Figure 2c). After chitin and sebocyte supernatant treatment, induction of TSLP mRNA could be non-significantly triggered. Of the used lipid components, palmitic acid, oleic acid and linoleic acid upregulated TSLP gene expression, but only linoleic acid could elevate it significantly. Further, we showed that linoleic acid induces TSLP mRNA expression in a concentration dependent manner, reaching its maximum and significantly higher level at 150 μM (Figure 2d and e). On the other hand, the basal TSLP protein levels could not be elevated by any of the aforementioned agents (Figure 2a-c). As sebum components influenced prominently TSLP expression in HaCaT cells, these experiments were repeated in NHEKs and similarly linoleic acid could dose-dependently elevate TSLP mRNA levels (Figure 2f and g). No TSLP protein secretion by NHEKs could be detected (not shown). It has previously been found in AD skin that barrier damage can also lead to TSLP production by KCs (Mocsai et al., 2014); therefore, transepidermal water loss and skin pH, representing barrier functions, were measured on SGP and SGR skin regions. No differences were detected, indicating that barrier damage is most probably not the cause of distinct TSLP production in SGR and SGP skin (not shown).

SGR skin is characterized by an elevated number of DCs without prominent activation and maturation compared to SGP skin

The significantly higher TSLP level of SGR skin suggested that differences in other immune surveillance factors may also exist. Since DCs are the major target cells of TSLP, CD11c+ dermal myeloid DCs and CD1a+ Langerhans cells (LCs) were immunolabeled and quantified

in SGR and SGP skin samples. IHC revealed that CD11c+ DCs were present in significantly higher numbers (Figure 3a and d) in SGR skin compared to SGP skin and the majority of these cells were characteristically localized near to sebaceous glands or the duct of the glands. In AD skin DC count was higher compared to SGR skin and DCs were found to be diffusely infiltrated in the dermis (Figure 3a and d). In contrast, no significant differences were found between the LC counts of SGP and SGR skin samples (Figure 3g and see Supplementary Figure S1a online).

To further analyze the characteristics of DCs, their classical maturation and/or activation markers CD80, CD83, CD86 and DC-LAMP were investigated on mRNA level. As the classical proinflammatory effect of TSLP is to boost Th2 polarizing DCs in allergic diseases, TARC [also known as Chemokine (C-C motif) ligand 17 (CCL17)], an atopic eczema specific, DC secreted chemokine, and CD83 were also assessed by IHC. Although the number of CD83 positive cells (Figure 3c and f) and mRNA levels of CD80 (Figure 3h), CD83 (Figure 3i), CD86 (Figure 3k) and LAMP3 (CD208) (Figure 3j) could be found in somewhat higher amounts in SGR skin compared to SGP, none of the investigated markers' expression differed significantly; while significantly higher numbers of CD83+ cells were detectable in AD samples (Fig 3c and f). TARC was completely absent from both types of healthy skin, but was present in AD samples (Figure 3b and e).

Elevated T cell number and non-inflammatory IL17/IL-10 cytokine milieu feature SGR skin

Next, CD3+ and CD4+ cells were stained in SGR and SGP skin samples. CD3+ (Figure 4a and d) and CD4+ (Figure 4b and e) T cells were present in significantly higher numbers in SGR skin compared to SGP skin. The localization of T cells was similar to that of DCs and the clear majority of T cells were Th cells.

As a next step, representative cytokines of Th subsets [IL-10: regulatory T cell (Treg); IL-13: Th2; IL-17: Th17 and interferon-γ (IFN-γ): Th1] were immunostained. IHC revealed that no IL-13+ and IFN-γ+ cells could be detected in either of the healthy skin types. IL-10+ and IL-17+ cells showed similar patterns; they were detected at very low levels or absent from SGP skin, but were found at significantly higher levels in SGR skin (Figure 5a-d and see Supplementary Figure S1b-e online). RT-PCR analyses of the aforementioned cytokines were also performed and showed a similar pattern to that found at the protein levels, although the differences were not significant (Figure 5e-h). In SGP skin the cytokine content was very low, in contrast to the characteristic IL-17/IL-10 cytokine milieu of SGR skin.

Then, the mRNA levels of transcription factors characteristic of different Th cell subsets were investigated. Expression of T-bet (TBX21 gene), mediating inflammatory Th17 [Th17(23)] and Th1 cell responses (Figure 5i) and GATA3, mediating Th2 responses (Figure 5j), were detected at similar levels in SGP and SGR skin. On the other hand, RORγt (RORC gene), mediating non-inflammatory Th17 [Th17(β)] and Th17(23) development (Figure 5k) and FOXP3, characteristic of Tregs (Figure 5l), showed notably higher expression levels in SGR compared to SGP skin. CCR4 (Figure 5m) and CCR8 (Figure 5n) mRNA levels, typical skin homing receptors of Tregs, were also detected in notably, but non-significantly higher levels in SGR skin compared to SGP (Geginat et al., 2014; Nomura et al., 2014).

Macrophage, neutrophil, eosinophil and mast cell counts are similar in SGR and SGP skin

To determine whether the numbers of macrophages, neutrophils, eosinophils and mast cells differ in SGP and SGR skin, anti-CD163 (macrophage labeling) and May-Grünwald-Giemsa (MGG) staining were performed. Examining the overall view of the skin sections, no significant differences could be detected in the above mentioned cell counts between SGR and SGP skin areas, although CD163+ macrophages were found in higher numbers in SGR

skin (Figure 4c and f). Neither neutrophils nor eosinophils were present in healthy skin regions, whereas mast cells were found in low numbers in both SGR and SGP skin samples (Figure 4g and see Supplementary Figure S1f online).

Papulopustular rosacea is characterized by significantly decreased TSLP level, elevated DC count and activity, robust influx of T cells and innate immune cells and an inflammatory IL-17/IFN-γ cytokine profile

To investigate the alterations of the characteristic immune surveillance of SGR skin in an inflammatory disease typically occurring in that skin region, papulopustular rosacea (PPR) samples were analyzed. Epidermal (Figure 1a and b) and stratum corneum (Figure 1c) TSLP protein levels were significantly decreased in PPR samples compared to SGR skin. The loss of the protein was not homogenous, but discontinuous through PPR epidermis. In contrast, no differences in its mRNA levels were found (Figure 1d). Infiltrating CD11c+ DCs (Figure 3a and d), CD3+ and CD4+ T cells (Figure 4a, b, d and e) were detected in significantly higher numbers in PPR compared to SGR skin and were present diffusely through the dermis. CD80, CD83, DC-LAMP and CD86 activation and/or maturation markers of DCs (Figure 3h-k) were all significantly upregulated on mRNA levels compared to SGR skin. Although CD83+ DCs were present in significantly elevated numbers (Figure 3c and f), TARC positivity was almost undetectable in PPR skin (Figure 3b and e). Moreover, strong, but non-significant correlation was detected between the increase of DC count and the decrease of TSLP level in PPR samples (Figure 3l). No difference was found between SGR and PPR skin regarding the number of LCs (Figure 3g and see Supplementary Figure S1a online). Significantly higher numbers of macrophages, mast cells and neutrophils could be detected in PPR skin compared to SGR, while eosinophils were absent from both SGR and PPR samples (Figure 4c, f, g and see Supplementary Figure S1f online).

The characterization of cytokine milieu was also performed in PPR skin samples. Parallel to the prominent increase in the number of IL-10+ and IL-17+ cells in PPR compared to SGR skin samples, an especially robust IFN-γ+ cell presence was detected, while IL-13+ cells were absent (Figure 5a-d and see Supplementary Figure S1b-e online). The mRNA levels of cytokines corresponded to their protein levels (Figure 5e-h). Gene expression levels of TBX21 (Figure 5i) and FOXP3 (Figure 5l) were significantly higher in PPR compared to SGR skin, while RORC (Figure 5k) and GATA3 (Figure 5j) gene expression levels were lower than in healthy SGR skin. Expressions of both Treg homing receptors (CCR4 and CCD8) were significantly higher in PPR samples than in SGR skin (Figure 5m and n).

DISCUSSION

Skin microbial community exhibits remarkable differences on seborrheic, dry and moist regions probably connected to the different physiology of these sites (Grice et al., 2009; Grice and Segre, 2011). Since skin microbiota has mutualistic connection with the skin immune system (Belkaid and Segre, 2014; Belkaid and Tamoutounour, 2016; Grice and Segre, 2011; Naik et al., 2015), possible immunological distinctions between topographically different healthy skin sites can be postulated but have not been revealed.

Previous investigations on the immune activity of intestinal mucosa indicated distinct presence of TSLP in particular gut sections, thus, in our study, TSLP, also an important cytokine of KCs, was studied first (Rimoldi et al., 2005; Swamy et al., 2010). A constitutive TSLP protein expression was detected by two methods (IHC and immunocytochemistry) in healthy SGR skin areas; in contrast, in healthy SGP areas TSLP was practically absent. Although TSLP mRNA expression has already been detected in healthy skin, its protein expression (Bjerkan et al., 2015; Fornasa et al., 2015) was found only in inflamed epidermis (AD, psoriasis) until now (Soumelis et al., 2002; Ziegler, 2012). The conflicting data between the previous publications and our current study might be explained by that the other investigators most probably used healthy SGP skin and no SGR samples as controls of AD or psoriasis.

Although the protein expression of TSLP showed remarkable differences between healthy SGP and SGR skin, mRNA levels were similar in all samples. The discrepancy between the protein and mRNA expressions of TSLP can be explained by important, but presently unknown posttranscriptional modifications during KC differentiation. Bogiatzi et al. detected a basal TSLP mRNA expression without the presence of the protein in cultured KCs, and this mRNA content was not upregulated in the presence of proallergic cytokines (Bogiatzi et al., 2007). On the other hand, when whole skin explant, a model that preserves the differentiation

of KCs, was used, TSLP protein could be measured after cytokine incubation (Bogiatzi et al., 2007). The importance of the posttranscriptional modifications can also explain our observations that, although linoleic acid could significantly and dose-dependently elevate TSLP mRNA levels, protein production was not increased. Until now, no study investigated the effect of sebum components and SZ95 sebocyte supernatant on TSLP mRNA and protein expression of cultured or HaCaT KCs and only one research group examined the outcome of chitin treatment on primary and HaCaT KCs' TSLP protein production (Koller et al., 2011). Although mRNA levels were not investigated, the authors detected significantly elevated TSLP protein levels in a concentration-dependent manner, which observation could not be confirmed by us. Nevertheless, according to our results sebum lipid content may have a role in the initiation of TSLP production in SGR skin.

Since DCs are the major target cells of TSLP action, the significantly higher TSLP levels of SGR skin proposed that differences in other immune surveillance factors may also exist between SGR and SGP areas. Although no difference was found in the LC count, the number of CD11c+ DCs was significantly elevated in SGR skin compared to SGP areas. Despite their high number, DCs did not exhibit noticeable activity. Moreover, the complete absence of TARC+ cells indicates that TSLP expressed by SGR skin does not act as it is described in AD skin, where TSLP induces TARC+ DCs promoting Th2 responses (Soumelis et al., 2002). The fact that TSLP has not only an inflammatory, but also a tolerogenic function (especially in lower amounts) on DCs is known from immunological studies of the gut (Zeuthen et al., 2008; Ziegler and Artis, 2010). A plethora of evidence supports the crucial role of TSLP in the maintenance of intestinal immune homeostasis and tolerance to commensal flora (Rimoldi et al., 2005; Zaph et al., 2007). We propose that TSLP found in SGR skin might have a similar role, since i) SGR skin samples were clinically healthy without any signs of

inflammation; ii) the amount of TSLP was lower than found in AD samples; and iii) DCs were TARC negative without noticeable activation.

We also examined and found differences between SGR and SGP skin sites regarding the number of T cells and levels of cytokines, as well as transcription factors characteristic to different Th subsets. Significantly more T cells were present in SGR skin, which cells were dominantly Tregs and probably also Th17(β) cells. The presence of Tregs was proven by the higher expression of FOXP3 and CCR4 as well as CCR8 Treg homing receptors accompanied by significantly higher IL-10+ cell counts. According to recent data, about 20% of CD4+ cells in healthy human skin express FOXP3 and these Tregs are effector memory cells being associated with hair follicles (Nomura et al., 2014; Sanchez Rodriguez et al., 2014); however, these authors did not compare different topographical skin sites. The higher Treg content detected in our study was also supported by a recent clinical investigation; i.e. skin metastases from solid-organ tumors were found most commonly on head and neck areas, and the authors also hold the higher number of Tregs responsible for the higher probability of metastases on these sites (Schulman et al., 2016).

Recently Th17 cells were divided in non-pathogenic Th17(β) and pathogenic Th17/Th23(23) cells. Th17(β) cells are characterized by IL-17 and IL-10 production and the expression of RORγt, while Th17(23) cells play an important role in the development of inflammatory and autoimmune diseases, produce IL-17, INF-γ and GM-CSF and express T-bet and RORγt transcription factors (Geginat et al., 2014; Nomura et al., 2014). Although significantly more IL-17+ and IL-10+ cells were present in SGR skin, IFN-γ+ cells were completely absent, and besides the higher RORγt expression, T-bet mRNA levels did not differ compared to SGP skin. Therefore, we suppose that non-pathogenic Th17(β) cells were detected in SGR skin (Geginat et al., 2014; Nomura et al., 2014). Innate lymphoid cells and γδT cells must also be taken into consideration as they are known to produce IL-17 (Sutton et

al., 2012). The non-inflammatory T cell milieu of SGR skin was also supported by the similarly low appearance of innate immune cells in both healthy skin areas.

In conclusion, our results suggest that similar to skin microbiota and chemical milieu, a fine topographical difference does exist in the activity of the human skin immune system regarding an epidermal factor (TSLP), DCs and T cells, although in this study moist skin regions were not investigated (manuscript under preparation). These results hence may provide explanation of the characteristic localization of certain immune-mediated skin diseases in special topographical skin areas (i.e. AD on SGP and PPR on SGR skin sites). Moreover, our data highlight the importance of correctly used topologically identical control skin samples in scientific studies. Further, our study may influence future barrier repair therapeutic approaches.

After detecting this special immune surveillance in healthy SGR skin, we wondered how this can be changed in an immune mediated skin disease like PPR, which is exclusively localized to SGR skin regions. In PPR, special activation of both the innate and adaptive immune mechanisms were previously described despite the absence of an obvious infectious or dangerous trigger, and literature suggests that decreased tolerance could be responsible for this increased skin sensitivity.

According to our findings, in PPR skin, TSLP was lost, DCs became activated, T cells turned to inflammatory type [Th1 and Th17(23)] and their numbers were highly elevated, similarly to a recent study (Buhl et al., 2015), resulting in the disruption of the non-inflammatory immune milieu of SGR skin. Although Treg presence was also higher, this is not a contradiction, as their accumulation was usually detected in inflammatory skin diseases (Nomura et al., 2014). These changes were accompanied by the significant influx of macrophages, neutrophils and mast cells. We were also able to show that linoleic acid, an important component of sebum, exerted an effect on TSLP expression; moreover, literature

data described altered sebum composition in rosacea patients (Ni Raghallaigh et al., 2012; Two et al., 2015). Based on these findings we hypothesize that this altered sebum production in rosacea and the consequently occurring loss of tolerogenic TSLP may be one of the main events during PPR development (Figure 6). This change in TSLP level may influence DC and T cell activation (Kinoshita et al., 2009; Spadoni et al., 2012). At the same time, since DCs can potentially be exposed directly to changes of sebum, chemical milieu and microbiota of the skin, the disruption of the non-inflammatory milieu can also be initiated by DCs or T cells (Mittal et al., 2013; Naik et al., 2015).

MATERIALS AND METHODS

Skin biopsies

Skin punch biopsies (0.5-1 cm^2) were taken from lesional skin of 8 AD patients, from 10 patients with PPR, and from normal skin of 18 healthy individuals (8 from SGP and 10 from SGR skin sites; Table 1.) after obtaining written, informed consent, according to the Declaration of Helsinki principles. The study was approved by the local ethics committee of University of Debrecen, Hungary. All biopsies were cut in two pieces. For IHC, samples were paraffin-embedded, whereas for RT-PCR, samples were stored in RNAlater (Qiagen, Hilden, Germany) at -70°C until RNA isolation. After haematoxylin and eosin (H&E) staining, samples were sorted according to the number of sebaceous glands and were defined as SGP skin when containing $n \leq 1$ sebaceous glands and as SGR skin when containing $n \geq 3$ sebaceous glands in the field of view on 10 x magnification in the microscope (Table 1).

Cell culture

HaCaT and NHEK KCs and SZ95 sebocytes (Zouboulis et al., 1999) were cultured and seeded at 50000 cells/well in 12-well plates for further RT-PCR and cytokine ELISA measurements. For a detailed description, see Supplementary Methods online.

RNA isolation and quantitative real-time PCR

RNA was extracted from the skin tissue specimens and HaCaT KCs with Tri Reagent (Sigma-Aldrich, Dorset, UK) and converted to cDNA by using the High Capacity cDNA Archive Kit (Invitrogen, Life Technologies, San Francisco, CA). Levels of TSLP, CD80, CD83, CD86, LAMP3, IL-10, IL-13, IL-17A, IFN-γ, TBX21, GATA3, RORC, FOXP3, CCR4 and CCR8 transcripts were also examined by using pre-designed MGB assays ordered from Applied Biosystems (Life Technologies). For a detailed description, see Supplementary Methods online.

Immunohistochemistry, routine staining and whole-slide imaging

Paraffin-embedded sections were stained with antibodies (Ab) against human TSLP (3 different Abs), CD3, CD4, CD1a, CD11c, CD163, CD83, TARC, IL-10, IL-13, IL-17 and IFN-γ. Skin specimens were also stained with H&E and MGG. The slides were digitalized and analyzed by using Pannoramic Viewer 1.15.2 (3DHistech Ltd, Budapest, Hungary) software. For a detailed description, see Supplementary Methods online.

Stratum corneum TSLP measurement

The tape-stripping method and immunostaining were carried out according to the method described in a previous report (Morita et al., 2010). For a detailed description, see Supplementary Methods online.

ELISA

The concentration of TSLP in the supernatant was quantified in triplicates by using anti-human TSLP Quantikine® enzyme-linked immunosorbent assay (ELISA) (R&D Systems).

Measurement of transepidermal water loss and skin pH

For a detailed description, see Supplementary Methods online.

Statistical analysis

To determine the statistical significance between the groups, one-way analysis of variance (ANOVA) test and Newman-Keuls post test were used. Differences between the groups were demonstrated using MEAN ± SEM. P-values <0.05 were considered statistically significant (*$p<0.05$; **$p<0.01$; ***$p<0.001$). Analysis of correlations was performed by Pearson r test. Two-tailed P values <0.05 were considered statistically significant (*$p<0.05$, **$p<0.01$).

CONFLICT OF INTEREST

The authors state no conflict of interest.

ACKNOWLEGMENTS

The research leading to these results has received funding from the Hungarian Research Grant (OTKA-K108421 and OTKA-PD 112077). DT was supported through the New National Excellence Program of the Ministry of Human Capacities.

REFERENCES

Belkaid Y, Segre JA. Dialogue between skin microbiota and immunity. Science 2014;346:954-9.

Belkaid Y, Tamoutounour S. The influence of skin microorganisms on cutaneous immunity. Nat Rev Immunol 2016;16:353-66.

Bjerkan L, Schreurs O, Engen SA, Jahnsen FL, Baekkevold ES, Blix IJ, et al. The short form of TSLP is constitutively translated in human keratinocytes and has characteristics of an antimicrobial peptide. Mucosal Immunol 2015;8:49-56.

Bogiatzi SI, Fernandez I, Bichet JC, Marloie-Provost MA, Volpe E, Sastre X, et al. Cutting Edge: Proinflammatory and Th2 cytokines synergize to induce thymic stromal lymphopoietin production by human skin keratinocytes. J Immunol 2007;178:3373-7.

Bouslimani A, Porto C, Rath CM, Wang M, Guo Y, Gonzalez A, et al. Molecular cartography of the human skin surface in 3D. Proc Natl Acad Sci U S A 2015;112:E2120-9.

Buhl T, Sulk M, Nowak P, Buddenkotte J, McDonald I, Aubert J, et al. Molecular and morphological characterization of inflammatory infiltrate in rosacea reveals activation of Th1/Th17 Pathways. J Invest Dermatol 2015;135:2198-208.

Costello EK, Lauber CL, Hamady M, Fierer N, Gordon JI, Knight R. Bacterial community variation in human body habitats across space and time. Science 2009;326:1694-7.

Eckburg PB, Bik EM, Bernstein CN, Purdom E, Dethlefsen L, Sargent M, et al. Diversity of the human intestinal microbial flora. Science 2005;308:1635-8.

Fornasa G, Tsilingiri K, Caprioli F, Botti F, Mapelli M, Meller S, et al. Dichotomy of short and long thymic stromal lymphopoietin isoforms in inflammatory disorders of the bowel and skin. J Allergy Clin Immunol 2015;136:413-22.

Gao Z, Tseng CH, Pei Z, Blaser MJ. Molecular analysis of human forearm superficial skin bacterial biota. Proc Natl Acad Sci U S A 2007;104:2927-32.

Geginat J, Paroni M, Maglie S, Alfen JS, Kastirr I, Gruarin P, et al. Plasticity of human CD4 T cell subsets. Front Immunol 2014;5:630.

Grice EA, Kong HH, Conlan S, Deming CB, Davis J, Young AC, et al. Topographical and temporal diversity of the human skin microbiome. Science 2009;324:1190-2.

Grice EA, Segre JA. The skin microbiome. Nat Rev Microbiol 2011;9:244-53.

He R, Geha RS. Thymic stromal lymphopoietin. Ann N Y Acad Sci 2010;1183:13-24.

Kinoshita H, Takai T, Le TA, Kamijo S, Wang XL, Ushio H, et al. Cytokine milieu modulates release of thymic stromal lymphopoietin from human keratinocytes stimulated with double-stranded RNA. J Allergy Clin Immunol 2009;123:179-86.

Koller B, Muller-Wiefel AS, Rupec R, Korting HC, Ruzicka T. Chitin modulates innate immune responses of keratinocytes. PLoS One 2011;6:e16594.

Maranduba CM, De Castro SB, de Souza GT, Rossato C, da Guia FC, Valente MA, et al. Intestinal microbiota as modulators of the immune system and neuroimmune system: impact on the host health and homeostasis. J Immunol Res 2015;2015:931574.

Mittal A, Raber AS, Schaefer UF, Weissmann S, Ebensen T, Schulze K, et al. Non-invasive delivery of nanoparticles to hair follicles: a perspective for transcutaneous immunization. Vaccine 2013;31:3442-51.

Mocsai G, Gaspar K, Nagy G, Irinyi B, Kapitany A, Biro T, et al. Severe skin inflammation and filaggrin mutation similarly alter the skin barrier in patients with atopic dermatitis. Br J Dermatol 2014;170:617-24.

Morita E, Takahashi H, Niihara H, Dekio I, Sumikawa Y, Murakami Y, et al. Stratum corneum TARC level is a new indicator of lesional skin inflammation in atopic dermatitis. Allergy 2010;65:1166-72.

Naik S, Bouladoux N, Linehan JL, Han SJ, Harrison OJ, Wilhelm C, et al. Commensal-dendritic-cell interaction specifies a unique protective skin immune signature. Nature 2015;520:104-8.

Ni Raghallaigh S, Bender K, Lacey N, Brennan L, Powell FC. The fatty acid profile of the skin surface lipid layer in papulopustular rosacea. Br J Dermatol 2012;166:279-87.

Nomura T, Kabashima K, Miyachi Y. The panoply of alphabetaT cells in the skin. J Dermatol Sci 2014;76:3-9.

Podolsky DK. The current future understanding of inflammatory bowel disease. Best Pract Res Clin Gastroenterol 2002;16:933-43.

Rimoldi M, Chieppa M, Salucci V, Avogadri F, Sonzogni A, Sampietro GM, et al. Intestinal immune homeostasis is regulated by the crosstalk between epithelial cells and dendritic cells. Nat Immunol 2005;6:507-14.

Round JL, Mazmanian SK. The gut microbiota shapes intestinal immune responses during health and disease. Nat Rev Immunol 2009;9:313-23.

Sanchez Rodriguez R, Pauli ML, Neuhaus IM, Yu SS, Arron ST, Harris HW, et al. Memory regulatory T cells reside in human skin. J Clin Invest 2014;124:1027-36.

Schulman JM, Pauli ML, Neuhaus IM, Sanchez Rodriguez R, Taravati K, Shin US, et al. The distribution of cutaneous metastases correlates with local immunologic milieu. J Am Acad Dermatol 2016;74:470-6.

Soumelis V, Reche PA, Kanzler H, Yuan W, Edward G, Homey B, et al. Human epithelial cells trigger dendritic cell mediated allergic inflammation by producing TSLP. Nat Immunol 2002;3:673-80.

Spadoni I, Iliev ID, Rossi G, Rescigno M. Dendritic cells produce TSLP that limits the differentiation of Th17 cells, fosters Treg development, and protects against colitis. Mucosal Immunol 2012;5:184-93.

Sutton CE, Mielke LA, Mills KH. IL-17-producing gammadelta T cells and innate lymphoid cells. Eur J Immunol 2012;42:2221-31.

Swamy M, Jamora C, Havran W, Hayday A. Epithelial decision makers: in search of the 'epimmunome'. Nat Immunol 2010;11:656-65.

Two AM, Wu W, Gallo RL, Hata TR. Rosacea: part I. Introduction, categorization, histology, pathogenesis, and risk factors. J Am Acad Dermatol 2015;72:749-58; quiz 59-60.

Zaph C, Troy AE, Taylor BC, Berman-Booty LD, Guild KJ, Du Y, et al. Epithelial-cell-intrinsic IKK-beta expression regulates intestinal immune homeostasis. Nature 2007;446:552-6.

Zeuthen LH, Fink LN, Frokiaer H. Epithelial cells prime the immune response to an array of gut-derived commensals towards a tolerogenic phenotype through distinct actions of thymic stromal lymphopoietin and transforming growth factor-beta. Immunology 2008;123:197-208.

Ziegler SF. Thymic stromal lymphopoietin and allergic disease. J Allergy Clin Immunol 2012;130:845-52.

Ziegler SF, Artis D. Sensing the outside world: TSLP regulates barrier immunity. Nat Immunol 2010;11:289-93.

Zouboulis CC, Seltmann H, Neitzel H, Orfanos CE. Establishment and characterization of an immortalized human sebaceous gland cell line (SZ95). J Invest Dermatol 1999;113:1011-20.

Table 1. Characteristics and TSLP protein expression in the skin of the studied individuals

Healthy individuals (HI)/Patients (P)	Sex	Age	Localization	Count of Sebaceous Glands	Intensity of TSLP staining (visual scoring)	Intensity of TSLP staining (Pannoramic Viewer software)
SGP skin (n=8)						
HI 1	M	77	Shin	-	+	1,50E-03
HI 2	M	85	Shin	-	-	7,01E-04
HI 3	F	72	Lower arm	-	-	6,43E-04
HI 4	F	81	Lower arm	-	-	5,70E-04
HI 5	M	40	Lower arm	-	-	6,86E-04
HI 6	F	72	Lower arm	-	+	1,30E-03
HI 7	F	86	Hand	-	-	8,90E-04
HI 8	F	56	Shin	-	-	2,70E-04
MEAN AGE ± SD		71,1 ± 15,8				
SGR skin (n=10)						
HI 9	F	77	Heary scalp	+	++	5,66E-03
HI 10	M	62	Mandibula	++	+++	6,72E-03
HI 11	F	57	Nose	+++	+++	9,18E-03
HI 12	F	61	Nose	+++	+++	6,72E-03
HI 13	F	42	Scapula	++	++	5,51E-03
HI 14	F	38	Chin	++	++	4,51E-03
HI 15	M	56	Shoulder	+++	++	4,91E-03
HI 16	M	47	Heary scalp	++	+++	9,90E-03
HI 17	F	19	Face (central part)	+++	+++	8,01E-03
HI 18	M	66	Face (lateral part)	+++	+++	7,07E-03
MEAN AGE ± SD		52,5 ± 16,8				
PPR skin (n=10)						
P 1	F	65	Face	+++	++	6,78E-03
P 2	F	71	Face	+++	-	9,18E-04
P 3	M	70	Nose	+++	-	1,03E-04
P 4	F	68	Face	+++	-	1,01E-03
P 5	F	57	Nose	+++	+	3,01E-03
P 6	M	69	Nose	+++	+	3,83E-03
P 7	M	66	Face	++	+	4,25E-03
P 8	M	67	Eyebrow	+++	++	6,41E-03
P 9	M	65	Forehead	++	+	3,79E-03
P 10	M	72	Eyebrow	++	+	4,56E-03
MEAN AGE ± SD		67,0 ± 4,3				

Table 1. Characteristics and TSLP protein expression in the skin of the studied individuals

Scoring of sebaceous gland count was performed according to the number and size of sebaceous glands in the field of view on 10 x magnification: samples containing $n \leq 1$ sebaceous gland were defined negative (-), containing $n \geq 3$ were defined positive and scored in accordance with the area of sebaceous glands in percentage of dermal surface: (+): 5-15%; (++): 15-30% and (+++): more than 30%. Visual scoring of TSLP staining was performed according to the percentage of the epidermal surface positively stained for TSLP: (-): 0-5%; (+): 5-15%; (++): 15-30% and (+++): more than 30%. PPR, papulopustular rosacea; SD, standard deviation; SGP, sebaceous gland poor; SGR, sebaceous gland rich; TSLP, thymic stromal lymphopoietin.

FIGURE LEGENDS

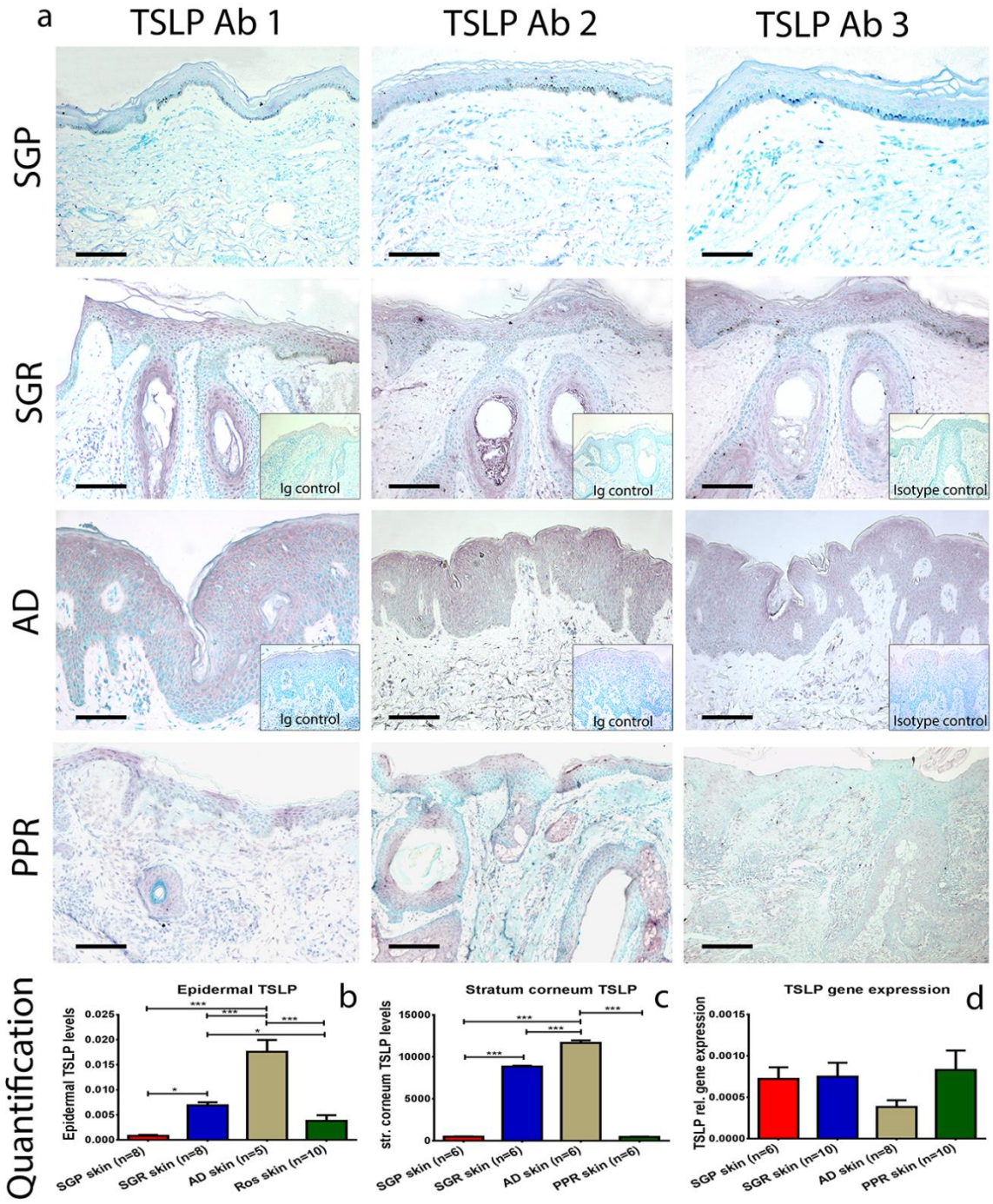

Figure 1. TSLP is absent from SGP skin, but constitutively expressed in SGR skin and attenuated in PPR skin. (**a**) Representative images for immunostaining of TSLP with 3 different TSLP antibodies (TSLP Ab 1: rabbit polyclonal anti-human TSLP Ab; TSLP Ab 2: sheep polyclonal anti-human TSLP Ab; TSLP Ab 3: mouse monoclonal anti-human TSLP

Ab) in SGP, SGR, AD and PPR skin sections. Size bars = 100 μm. Ig or isotype controls are presented in the bottom right corner of SGR and AD samples. Quantification of (**b**) epidermal TSLP protein levels; (**c**) Stratum corneum TSLP protein levels and (**d**) TSLP mRNA levels. Graphs show the mean ± standard error of the means of measured protein and mRNA levels (*P < 0.05; **P < 0.01; ***P < 0.001, as determined by one-way ANOVA followed by Newman-Keuls test). Ab, antibody; AD, atopic dermatitis; ANOVA, analysis of variance; PPR, papulopustular rosacea; SGP, sebaceous gland poor; SGR, sebaceous gland rich; TSLP, thymic stromal lymphopoietin.

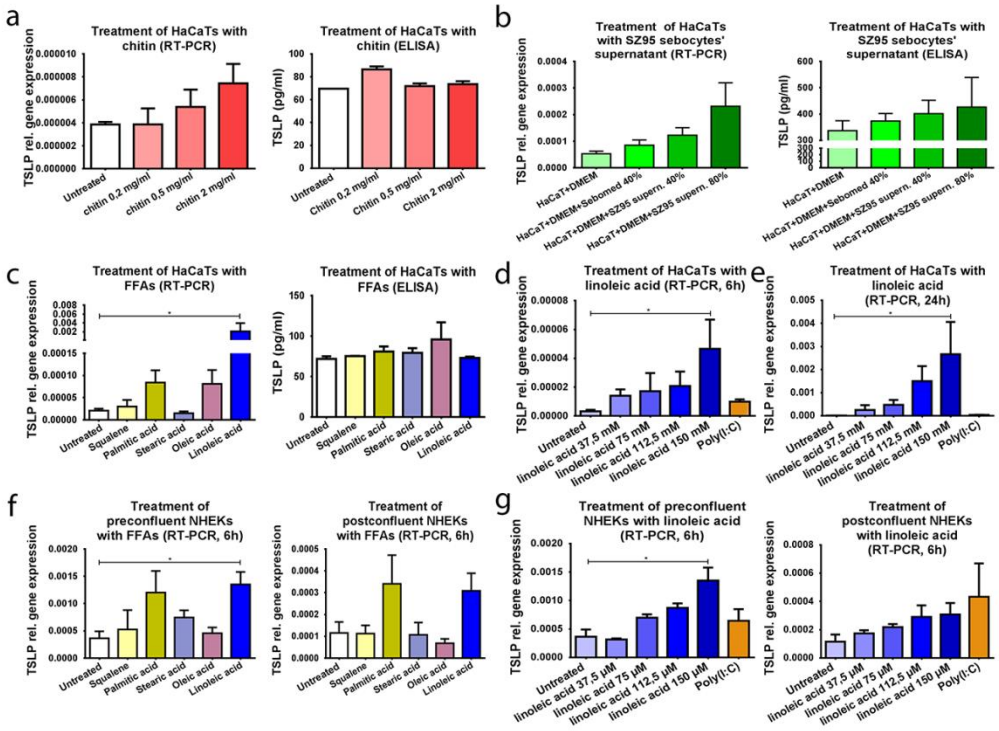

Figure 2. Linoleic acid upregulates TSLP gene expression in HaCaT keratinocytes. HaCaT KCs were incubated with (**a**) different chitin concentrations (0,2; 0,5 and 2 mg/ml), with (**b**) SZ95 sebocyte culture medium and SZ95 sebocyte supernatant (40% and 80%) and with (**c**) different sebum components, for 24 hours. Concentration-dependent effect of linoleic acid (37,5; 75; 112,5 and 150 µM) and Poly (I:C) after (**d**) 6h and **(e)** 24h treatment. TSLP mRNA levels were detected after treating pre- and postconfluent NHEK cells with different sebum components (**f**) and with different concentrations of linoleic acid (**g**) for 6 hours. No TSLP secretion of NHEKs could be detected by ELISA (not shown). Higher concentrations of linoleic acid than 150 µM highly decreased the viability of both cell types and incubation of NHEKs with linoleic acid for 24h had toxic effect. TSLP mRNA and protein levels were quantified by RT-PCR and ELISA. Graphs show the mean ± standard error of the means of measured protein and mRNA levels (*P < 0.05, as determined by one-way ANOVA followed by Newman-Keuls test). ANOVA, analysis of variance; ELISA, Enzyme-Linked Immunosorbent Assay; FFA, free fatty acid; RT-PCR, quantitative real-time PCR.

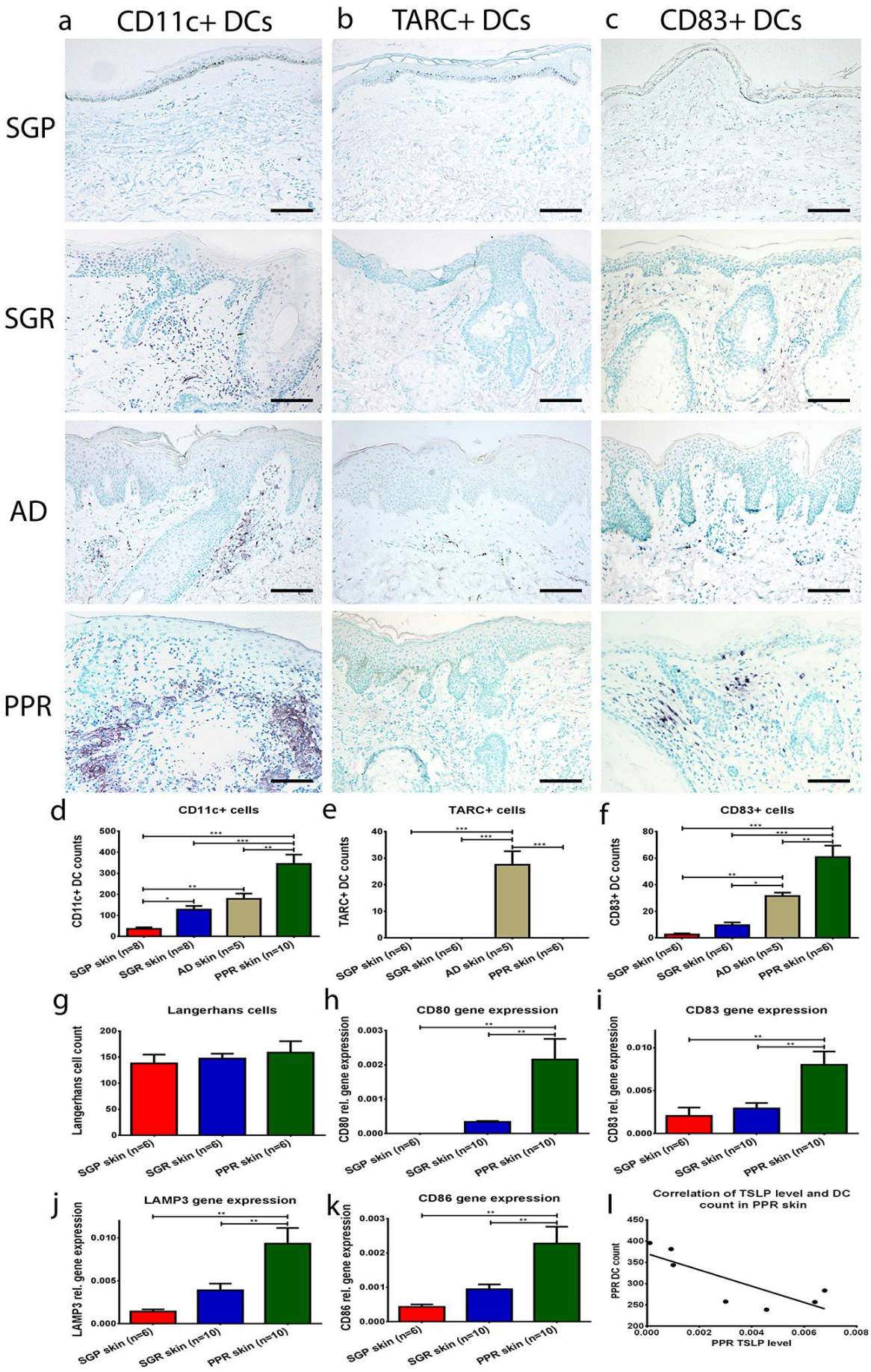
a CD11c+ DCs
b TARC+ DCs
c CD83+ DCs
SGP
SGR
AD
PPR
d
CD11c+ cells
CD11c+ DC counts
SGP skin (n=8)
SGR skin (n=8)
AD skin (n=5)
PPR skin (n=10)
e
TARC+ cells
TARC+ DC counts
SGP skin (n=6)
SGR skin (n=6)
AD skin (n=5)
PPR skin (n=6)
f
CD83+ cells
CD83+ DC counts
SGP skin (n=6)
SGR skin (n=6)
AD skin (n=5)
PPR skin (n=6)
g
Langerhans cells
Langerhans cell count
SGP skin (n=6)
SGR skin (n=6)
PPR skin (n=6)
h
CD80 gene expression
CD80 rel. gene expression
SGP skin (n=6)
SGR skin (n=10)
PPR skin (n=10)
i
CD83 gene expression
CD83 rel. gene expression
SGP skin (n=6)
SGR skin (n=10)
PPR skin (n=10)
j
LAMP3 gene expression
LAMP3 rel. gene expression
SGP skin (n=6)
SGR skin (n=10)
PPR skin (n=10)
k
CD86 gene expression
CD86 rel. gene expression
SGP skin (n=6)
SGR skin (n=10)
PPR skin (n=10)
l
Correlation of TSLP level and DC count in PPR skin
PPR DC count
PPR TSLP level

Figure 3. Elevated DC count with low activation state and without TARC positivity is detected in SGR skin. A robust influx of CD83+, TARC negative DCs is characteristic to PPR. Representative images for immunostaining of (**a**) CD11c, (**b**) TARC and (**c**) CD83 in SGP, SGR, AD and PPR skin sections. Size bars = 100 μm. Cell counts of (**d**) CD11c+ DCs, (**e**) TARC+ DCs, (**f**) CD83+ DCs and (**g**) Langerhans cells were blindly analyzed by Pannoramic Viewer software. Quantification of (**h**) CD80, (**i**) CD83, (**j**) LAMP3, and **(k)** CD86 mRNA levels by RT-PCR. **(l)** Strong, but not significant inverse correlation was found in PPR skin between TSLP level and DC count by Pearson r test (P=0.0526; Pearson r = -0.7219). Graphs show the mean ± standard error of the means of measured protein and mRNA levels (*P < 0.05; **P < 0.01; ***P < 0.001, as determined by one-way ANOVA followed by Newman-Keuls test). ANOVA, analysis of variance; AD, atopic dermatitis; LAMP3, lysosome-associated membrane glycoprotein 3; PPR, papulopustular rosacea; RT-PCR, quantitative real-time PCR; SGP, sebaceous gland poor; SGR, sebaceous gland rich; TARC, thymus and activation regulated chemokine

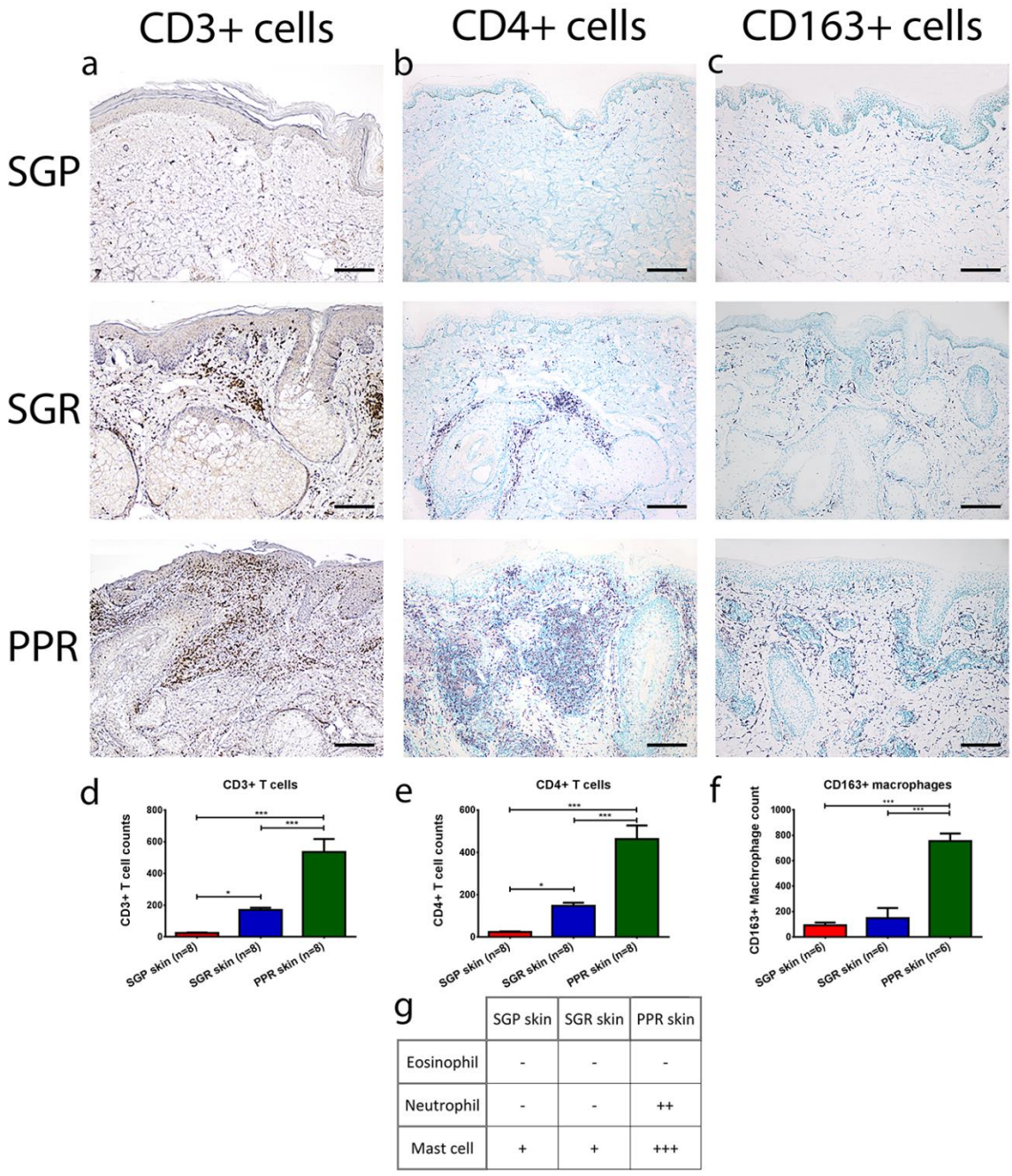

	SGP skin	SGR skin	PPR skin
Eosinophil	-	-	-
Neutrophil	-	-	++
Mast cell	+	+	+++

Figure 4. SGR skin sites are characterized by remarkable T cell presence and similar macrophage count compared to SGP skin. In PPR skin, robust influx of both cell types was observed. Representative images for immunostaining of (**a**) CD3, (**b**) CD4 and (**c**) CD163 in SGP, SGR and PPR skin sections. Cell counts of (**c**) CD3+, (**d**) CD4+ T cells and (**e**) CD163+ macrophages were blindly analyzed by Pannoramic Viewer software. Size bars = 100 μm. **(f)** Comparison of the presence of eosinophils, neutrophils and mast cells by

professional pathologist after May-Grünwald-Giemsa staining. Scoring system: (-) no cell observed; (+): low cell count; (++): moderate cell count; (+++): high cell count. Graphs show the mean ± standard error of the means of measured protein levels (*P < 0.05; **P < 0.01; ***P < 0.001, as determined by one-way ANOVA followed by Newman-Keuls test). ANOVA, analysis of variance; PPR, papulopustular rosacea; SGP, sebaceous gland poor; SGR, sebaceous gland rich.

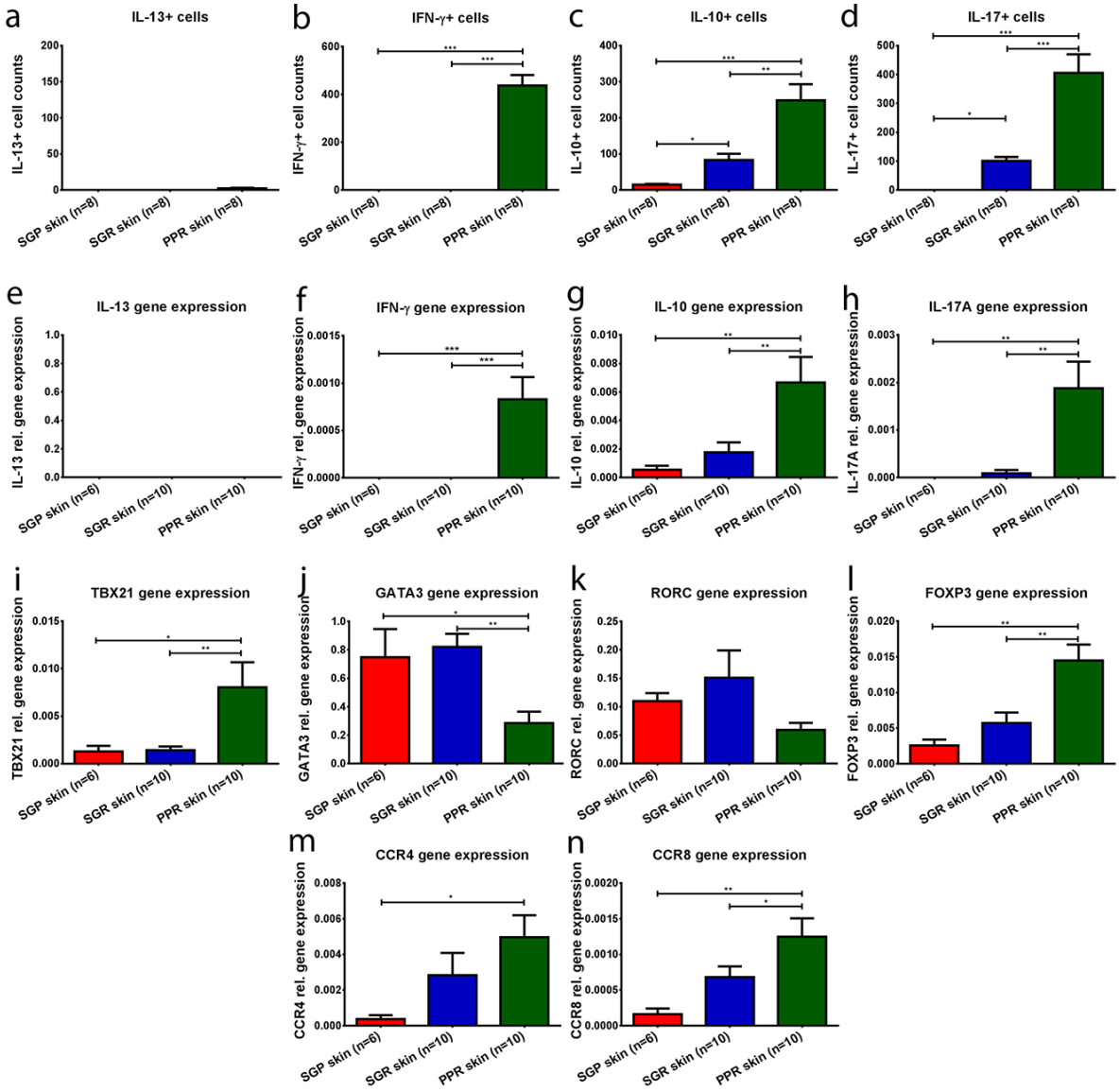

Figure 5. SGR skin sites, but not the SGP skin areas, are characterized by non-inflammatory IL-17/IL-10 milieu. In PPR skin, inflammatory IFN-γ/IL-17 cytokine milieu was observed. Cell counts of (**a**) IL-13+, (**b**) IFN-γ+, (**c**) IL-10+ and (**d**) IL-17+ cells

were blindly analyzed by Pannoramic Viewer software in SGP, SGR and PPR skin sections. Gene expression levels of **(e)** IL-13, **(f)** IFN-γ, **(g)** IL-10, **(h)** IL-17A cytokines and (**i**) TBX21, (**j**) GATA3, (**k**) RORC and (**l**) FOXP3 transcription factors and **(m)** CCR4 and **(n)** CCR8 Treg homing receptors detected by RT-PCR. Graphs show the mean ± standard error of the means of measured protein and mRNA levels. (*P < 0.05; **P < 0.01; ***P < 0.001, as determined by one-way ANOVA followed by Newman-Keuls test). ANOVA, analysis of variance; PPR, papulopustular rosacea; SGP, sebaceous gland poor; SGR, sebaceous gland rich.

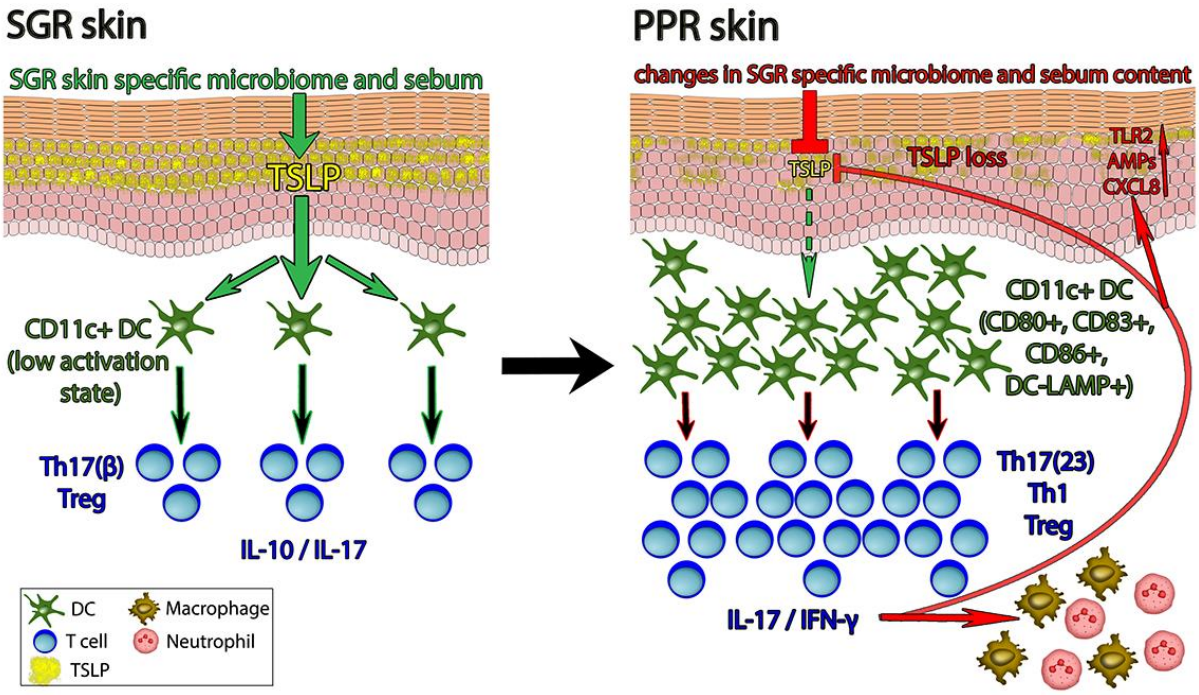

Figure 6. The disruption of special, non-inflammatory immune milieu of SGR skin may lead to the development of rosacea specific inflammation.

In the presence of TSLP produced by KCs, SGR skin infiltrating DCs are non-inflammatory and T cells are Tregs and Th17(β) cells. In PPR, altered sebum composition, decreased TSLP production, a plethora of inflammatory cells (DCs, T cells, macrophages, mast cells and neutrophils) and the disruption of the previous, non-inflammatory milieu are the characteristic features. In PPR, an IL-17/IFN-γ type [Th17(23), Th1] inflammation

develops, and since IL-17 is able to further inhibit TSLP expression, this can lead to a vicious circle. According to our results, we hypothesize that altered sebum composition could be responsible for the loss of tolerogenic TSLP, which may be one of the first steps in the disruption of the non-inflammatory milieu. AMP, antimicrobial peptide; CXCL8, chemokine (C-X-C motif) ligand 8; DC, dendritic cell; IFN-γ, interferon-γ; PPR, papulopustular rosacea; SGR, sebaceous gland rich; Th, T helper; Th17(β), non-pathogenic Th17 cell; Th17(23), pathogenic Th17 cell; TLR2, Toll-like receptor 2; Treg, regulatory T cell; TSLP, thymic stromal lymphopoietin.

SUPPLEMENTARY MATERIAL

Supplementary Figures

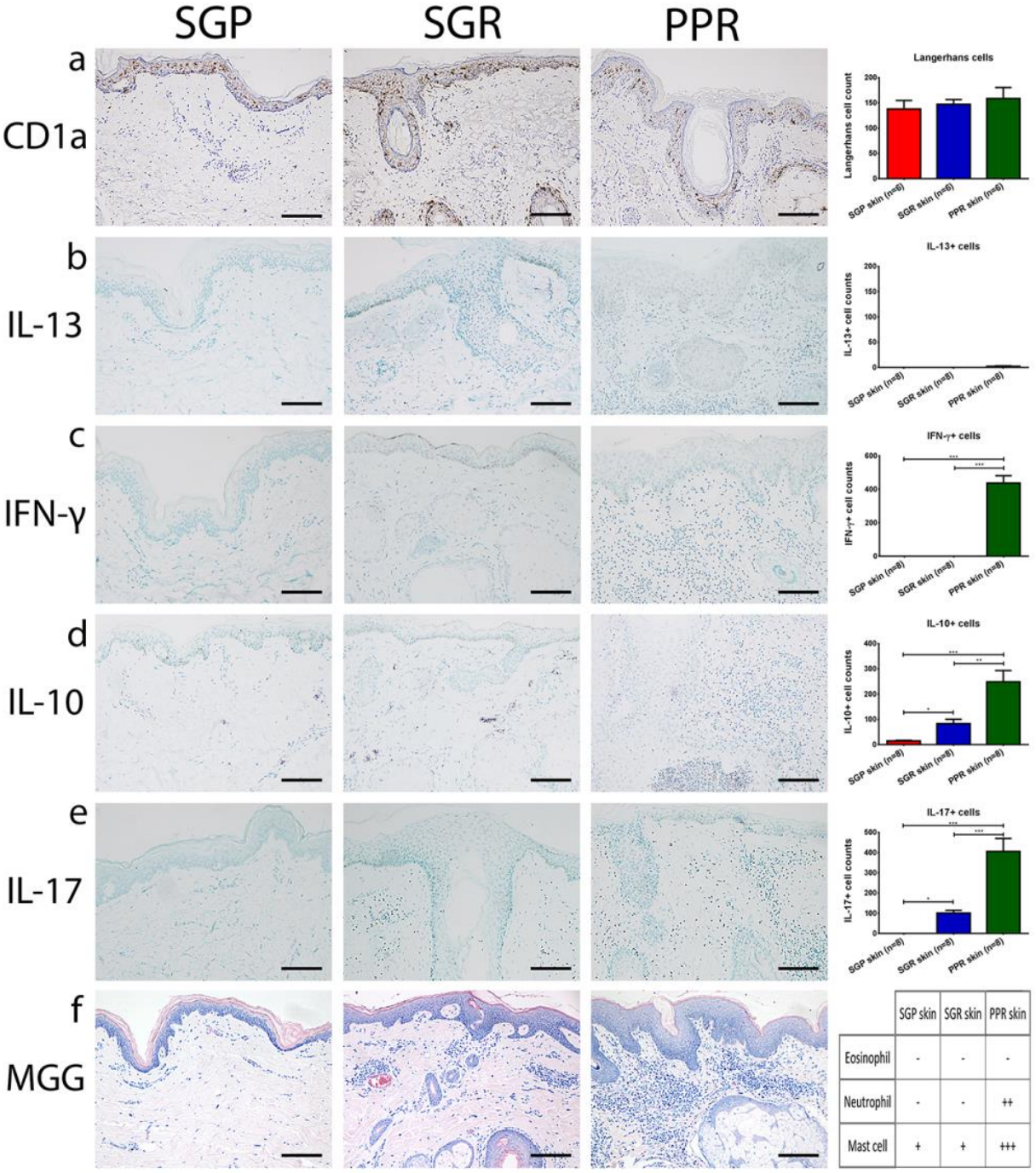

Supplementary Figure S1. SGR skin sites, but not the SGP skin areas, are characterized by non-inflammatory IL-17/IL-10 milieu. In PPR skin, inflammatory IFN-γ/IL-17 cytokine milieu was observed. Representative images and cell counts for immunostaining of (**a**) Langerhans cells, (**b**) IL-13+**,** (**c**) IFN-γ+ and (**d**) IL-10+ and **(e)** IL-17+ cells, blindly analyzed by Pannoramic Viewer software. **(f)** Comparison of the presence of eosinophils,

neutrophils and mast cells by professional pathologist after May-Grünwald-Giemsa staining. Scoring system: (-) no cell observed; (+): low cell count; (++): moderate cell count; (+++): high cell count. Size bars = 100 μm. Graphs show the mean ± standard error of the means of measured protein and mRNA levels. (*P < 0.05; **P < 0.01; ***P < 0.001, as determined by one-way ANOVA followed by Newman-Keuls test). ANOVA, analysis of variance; MGG, May-Grünwald-Giemsa; PPR, papulopustular rosacea; SGP, sebaceous gland poor; SGR, sebaceous gland rich.

Supplementary materials and methods

Cell culture

HaCaT KCs were cultured at 37°C in a humidified atmosphere containing 5%(v/v) CO_2, in Dulbecco Modified Eagle Medium (DMEM) (Thermo Scientific, Bioscience, Budapest, Hungary) supplemented with 10% Fetal Bovine Serum, 1% Antibioticum Mixture (Penicillin, Streptomycin, Neomycin) and 2mM glutamin (Sigma-Aldrich, Dorset, UK). Cells were seeded at 50 000 cells/well in 12-well plates for RT-PCR and cytokine ELISA measurements, and cultured until they reached 80% confluence, then the medium was changed. After further 24 hours of incubation, cells were treated for 6h or 24 h with different materials (Sebomed with or without SZ95 supernatant, chitin, free fatty acids (FFAs) (qualene, palmitic acid, stearic acid, oleic acid and linoleic acid).

NHEK cells were cultured at 37°C in a humidified atmosphere containing 5%(v/v) CO_2, in EpiLife® medium supplemented with HKGS (all from Gibco™, Thermo Fisher Scientific, Budapest, Hungary). Cells were seeded at 50 000 cells/well in 12-well plates for RT-PCR and cytokine ELISA measurements, and cultured until they reached preconfluency (70-80%) or postconfluency, then the medium was changed. After incubating preconfluent cells for 24 hours and postconfluent cells for 72 hours, cells were treated for 6h or 24 h with different materials (free fatty acids (FFAs) (qualene, palmitic acid, stearic acid, oleic acid and linoleic acid).

Human SZ95 sebocytes were cultured at 37°C in a humidified atmosphere containing 5%(v/v) CO_2, in Sebomed medium (Biochrom, Berlin, Germany) supplemented with 10% Fetal Bovine Serum, 1 mM $CaCl_2$ solution, 1% penicillin/streptomycin and 5 μg/ml Epidermal Growth Factor (EGF) (all from Sigma-Aldrich). Cells were kept in culture until reaching approximately 80% confluence. Prior to supernatant collection the used medium was replaced with Sebomed medium containing 0.5% Fetal Bovine Serum, 1 mM $CaCl_2$ solution, with or without 1% penicillin/streptomycin, lacking EGF. 24h supernatants were collected and

filtered using 0,2-µm syringe filters (Sarstedt, Nümbrecht, Germany) and used for experiments.

RNA isolation and quantitative real-time quantitative PCR

All samples were homogenized in Tri reagent solution (Sigma-Aldrich, Dorset, UK) with Tissue Lyser (QIAGEN) using previously autoclaved metal beads (QIAGEN), and total RNA was isolated from the human skin tissues and HaCaT and treated with DNase I (Applied Biosystems, Foster City, CA, USA) according to the manufacturer's instructions. The concentration and purity of the RNA were measured by means of NanoDrop spectrophotometer (Thermo Scientific, Bioscience, Budapest, Hungary), and its quality was checked using Agilent 2100 bioanalyser (Agilent Technologies, Santa Clara, CA, USA). For RT-PCR, cDNA was synthesized from the isolated RNA using the High Capacity cDNA Archive Kit (Invitrogen, Life Technologies, San Francisco, CA). RT-PCR was carried out in triplicate using pre-designed MGB assays ordered from Applied Biosystems (Life Technologies). The following primers were used: PPIA (Hs99999904_m1), TSLP (Hs00263639_m1), CD80 (Hs01045163_m1), CD83 (Hs00188486_m1), CD86 (Hs01567026_m1), LAMP3 (Hs00180880_m1), IL-13 (Hs00174379_m1), IL-10 (Hs00174086_m1), IL-17A (Hs00174383_m1), IFN-γ (Hs00174143_m1), TBX21 (Hs00203436_m1), GATA3 (Hs00231122_m1), RORC (Hs01076112_m1), FOXP3 (Hs01085834_m1), CCR4 (Hs00747615_s1) and CCR8 (Hs_00174764_m1). All reactions were performed with an ABI PRISM® 7000 Sequence Detection System. Relative mRNA levels were calculated using either the comparative CT or standard curve methods normalized to the expression of PPIA mRNA.

Immunohistochemistry and routine staining

For IHC analyses, paraffin-embedded sections from patients and healthy controls were deparaffinized. Heat-induced antigen retrieval was performed and sections were pre-processed with H_2O_2 for 10 minutes. Sections were stained with antibodies (Ab) against human TSLP (TSLP Ab 1: rabbit IgG [ab47943]: Abcam, Cambridge, UK; TSLP Ab 2: sheep polyclonal IgG [AF1398] (R&D Systems, MN, USA); TSLP Ab 3: mouse monoclonal IgG [MAB1398]: R&D Systems), human CD3 (rabbit polyclonal IgG [bs-0765R]: Bioss, MA, USA), human CD4 (rabbit monoclonal IgG [ab133616]: Abcam), human CD11c (rabbit monoclonal IgG [ab52632]: Abcam), CD1a (rabbit monoclonal IgG [ab108309]: Abcam), CD163 (rabbit monoclonal IgG [ALX-810-213]: Enzo, Farmingdale, NY, USA), CD83 (mouse monoclonal IgG [ab123494]: Abcam), TARC (goat polyclonal IgG [AF364]: R&D

Systems), human IL-10 (mouse monoclonal IgG [mab71148]: Covalab, Budapest, Hungary), human IL-13 (rabbit polyclonal IgG [bs-0560R]: Bioss), human IL17A (rabbit polyclonal IgG [pab70016]: Covalab) and human IFN-γ (mouse monoclonal IgG [mab30200]: Covalab). Subsequently, the following HRP-conjugated secondary Abs were employed: anti-mouse/rabbit (Dako), anti-sheep and anti-goat (R&D Systems). Before and after incubating with Abs, washing of samples was performed for 5 minutes, 3 times in each step. Staining was detected with the Vector VIP Kit (VECTOR Laboratories, Burlingame, CA, USA)/DAB (Dako). Sections were counterstained with methylene green or haematoxylin. The detection of one protein was carried out on all sections in parallel at the same time to enable us to evaluate comparable protein levels. Positive, Ig and isotype controls were also used to normalize staining against all proteins (mouse IgG2a Kappa [Covalab], sheep serum [Sigma-Aldrich], rabbit immunoglobulin fraction and goat serum [Dako]). Skin specimens were also stained with H&E and May–Grünwald–Giemsa. Visual scoring of TSLP, May-Grünwald-Giemsa staining and count of sebaceous glands was performed by professional pathologist.

Whole-slide imaging

The slides were digitalized using a Pannoramic SCAN digital slide scanner with a Zeiss plan-apochromat objective and Hitachi 3CCD progressive scan color camera. Immunostainings were analyzed with Pannoramic Viewer 1.15.2 (3DHistech Ltd., Budapest, Hungary), using the HistoQuant and NuclearQuant applications. Regions of interest (ROIs) (n=20/slide) were selected and then the Field area [FA (mm^2)] and the Mask area [MA (mm^2)] were measured by the software. The FA shows the whole area of the ROI, and the MA represents the positive area. The MA/FA values were counted for all ROIs. Measuring TSLP levels ROIs were selected according to two different methods. Relative (MA/FA) TSLP level was quantified as described above. Absolute TSLP level was measured as the quotient of FA and the epidermal length of the FA in each specimens. Important to mention that both methods showed the same result with smaller differences in relative TSLP levels due to the fact that acanthotic and thicker epidermis is characteristic to AD skin (smaller FA/MA value). Comparing the TSLP staining in the upper layer (approximately 50 μm, which corresponds to the thickness of healthy epidermis) of AD epidemis to healthy SGR epidermis, our result was similar to that we found in absolute TSLP levels (not shown).

Stratum corneum TSLP measurement

The tape-stripping method and immunostaining were carried out according to the method described in a previous report (Morita et al., 2010). Cells were incubated overnight with rabbit

anti-human TSLP primary Ab (AbCam) at 4°C. The cells were then incubated with Alexa-Fluor®-488-conjugated anti-rabbit IgG secondary Ab (goat; Life Technologies) for 2 h at room temperature. After being mounted, the cells were observed under a fluorescence microscope.

Measurement of transepidermal water loss and skin pH

Measurements were performed under standardized laboratory conditions at a temperature of 22–25°C and a humidity level of 40–60%. Before the measurements, individuals were allowed to adapt to the room conditions for 5 min. TEWL measurements (g/hm2) were carried out with Tewameter TM300 (Courage and Khazaka, Cologne, Germany) on the flexural forearm and on the face of individuals (n=50). The duration of the measurements, performed in triplicates, was 30 s. Skin pH measurements were carried out with pH 905 (Courage and Khazaka, Cologne, Germany) on the flexural forearm and the face of healthy individuals (n=50).